*Electromagnetic Wave Science and Technology*
https://www.sciltp.com/journals/ewst

*Supplementary Material*

# A Meta-Aramid-Based Composite with Strong Abrasion-Resistance Enabled by Sandwich and Brick-Mortar Architectures for Electromagnetic Shielding and Strain Sensing

Jiafei Wang [1,2], Rongjun Qu [1,*], Xinyu Li [1], Fang Ma [3], Ying Zhang [1], Jiaru Li [1], Liangfan Gong [1], Ying Wang [1], Changmei Sun [1,*], Xiquan Song [2,*], Qianli Ma [2], Xue Geng [2], Xiangyu Kong [2] and Ran An [2]

[1] School of Chemistry and Chemical Engineering, Ludong University, Yantai 264025, China
[2] Yantai Tayho Advanced Materials Co., Ltd., Yantai 264006, China
[3] College of Chemical Engineering and Technology, Yantai Nanshan University, Yantai 265713, China
* Correspondence: rongjunqu@sohu.com (R.Q.); sunchangmei0535@126.com (C.S.); ytaramid@163.com (X.S.)

**How To Cite:** Wang, J.; Qu, R.; Li, X.; et al. A Meta-Aramid-Based Composite with Strong Abrasion-Resistance Enabled by Sandwich and Brick-Mortar Architectures for Electromagnetic Shielding and Strain Sensing. *Electromagnetic Wave Science and Technology* **2026**, *1*(1), 1.

**This file includes:**

Supplementary Figure S1.
Supplementary Figure S2.
Supplementary Figure S3.
Supplementary Figure S4.
Supplementary Figure S5.
Supplementary Figure S6.
Supplementary Table S1.
Supplementary Table S2.
Supplementary Table S3.
Supplementary Table S4.

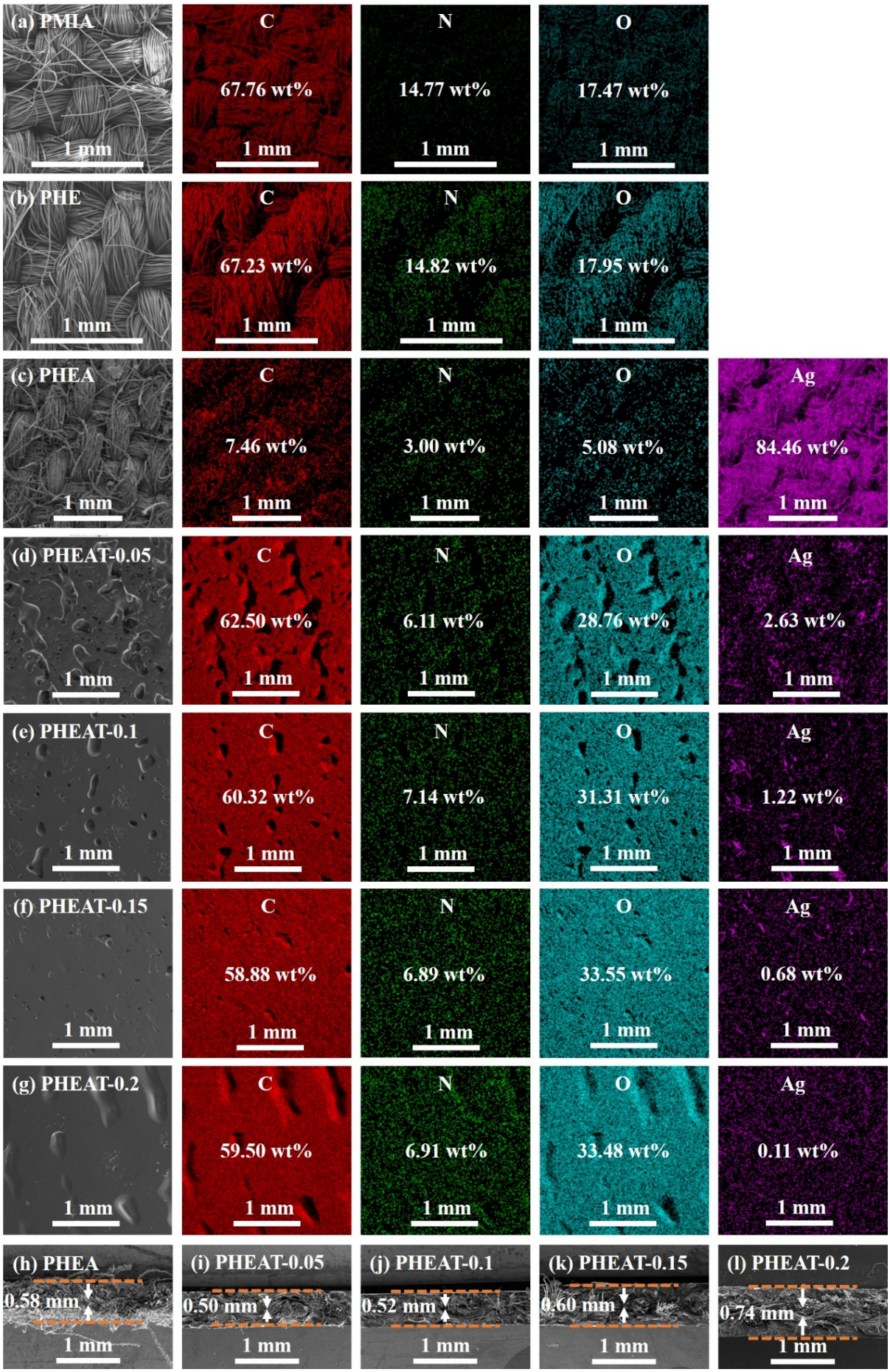


**Figure S1.** Microstructure of PMIA, PHE, PHEA and PHEAT. (**a**–**g**) SEM and corresponding C, N, O, Ag elemental mapping images; (**h**–**l**) SEM images demonstrating thickness.

The TPU film on the surface of PHEA underwent a film-melting-film transition process. Specifically, during hot-pressing, the TPU film softened into fluid and embedded into the inner surface region of the PHEA fabric. Upon cooling, the TPU combined together with PHEA fabric network, thereby enhancing the interaction between PHEA and TPU film. The cross-sectional SEM images of PHEAT is shown in Figure S1h–l. In PHEAT, the outer surface of PHEA fabric is encapsulated by TPU, which penetrates into the gaps of the fabric inner surface. The cured TPU forms a mechanical interlocking with the fabric, achieving good interfacial bonding.

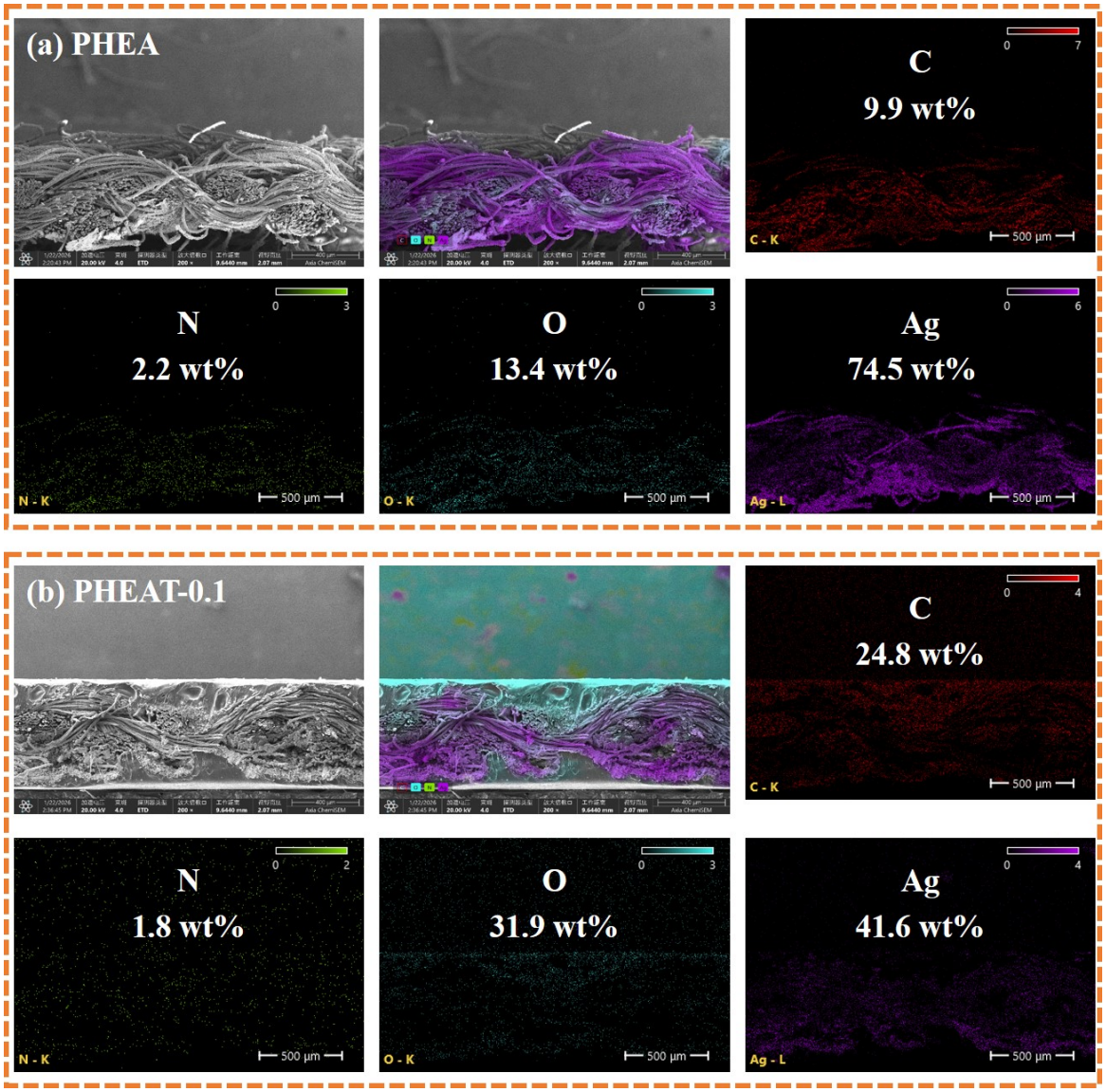


**Figure S2.** Microstructure of PHEA and PHEAT-0.1. Cross-sectional SEM and corresponding C, N, O, Ag elemental mapping images (**a**) PHEA (**b**) PHEAT-0.1.

Environmental stability: The reliability of PHEAT-0.05 and PHEAT-0.1 under harsh conditions was assessed using a HD-E702-408K40 humid & temp programmable tester (Haida International Equipment Co., Ltd., Dongguan, China) to simulate various humidity and temperature fluctuations according to GB/T 2423. That is, 5 groups of experiments were carried out separately, and the experimental parameters were 20 °C, 40% RH; 20 °C, 60% RH; 20 °C, 85% RH; 60% RH, 50 °C; 60% RH, 85 °C. After the experiment, the samples were dried to characterize the shielding performance. Additionally, the anti-oxidation and -environmental degradation was estimated after 6 months of storage.

Repeated washing: The bonding firmness of TPU film with PHEA fabric was evaluated using a SW-20E fabric textile washing color fastness testing machine (Meibang Instrument Co., Ltd., Quanzhou, China) following the China standard GB/T 3921-2008 with the following settings: bath ratio, 50:1; rotation speed, 40 rpm; temperature, 40 °C; washing time per cycle, 30 min. The PHEAT-0.05 and PHEAT-0.1 was fixed with two metal clips and placed in the test cup 10 steel beads with a diameter of 6 mm. After the experiment, the samples were dried to test the shielding performance.

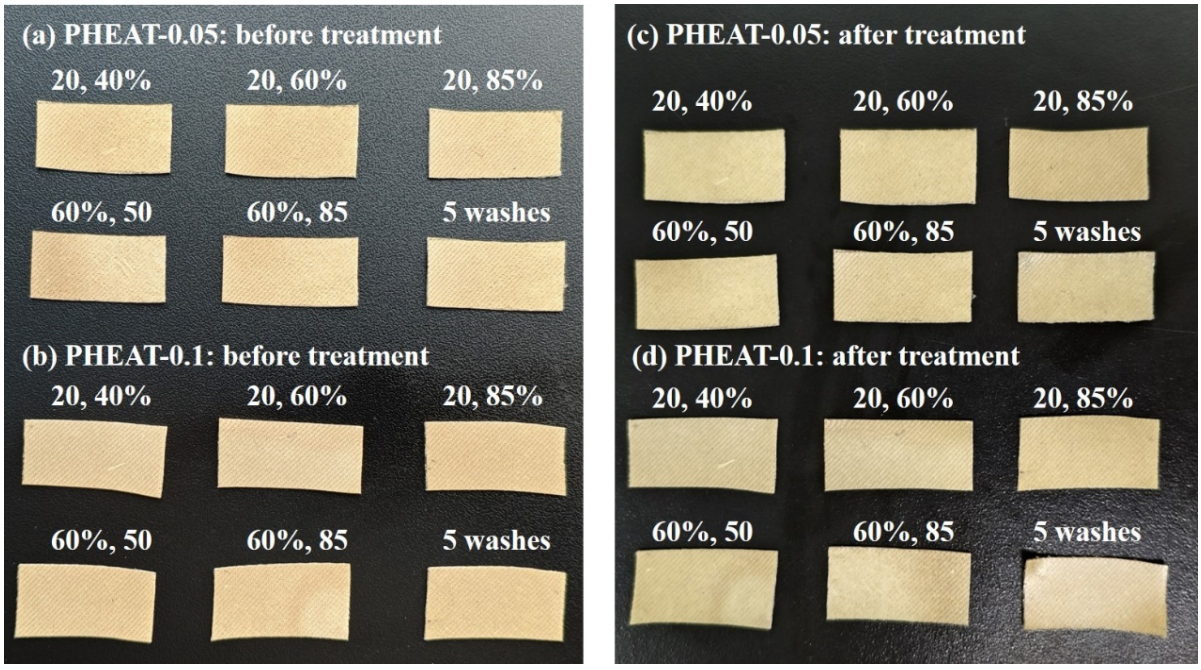


**Figure S3.** Environmental stability. Digital photos of (**a**,**c**) PHEAT-0.05 (**b**,**d**) PHEAT-0.1 before and after exposure to various temperature (°C) and relative humidity (RH), and 5 washing cycles.

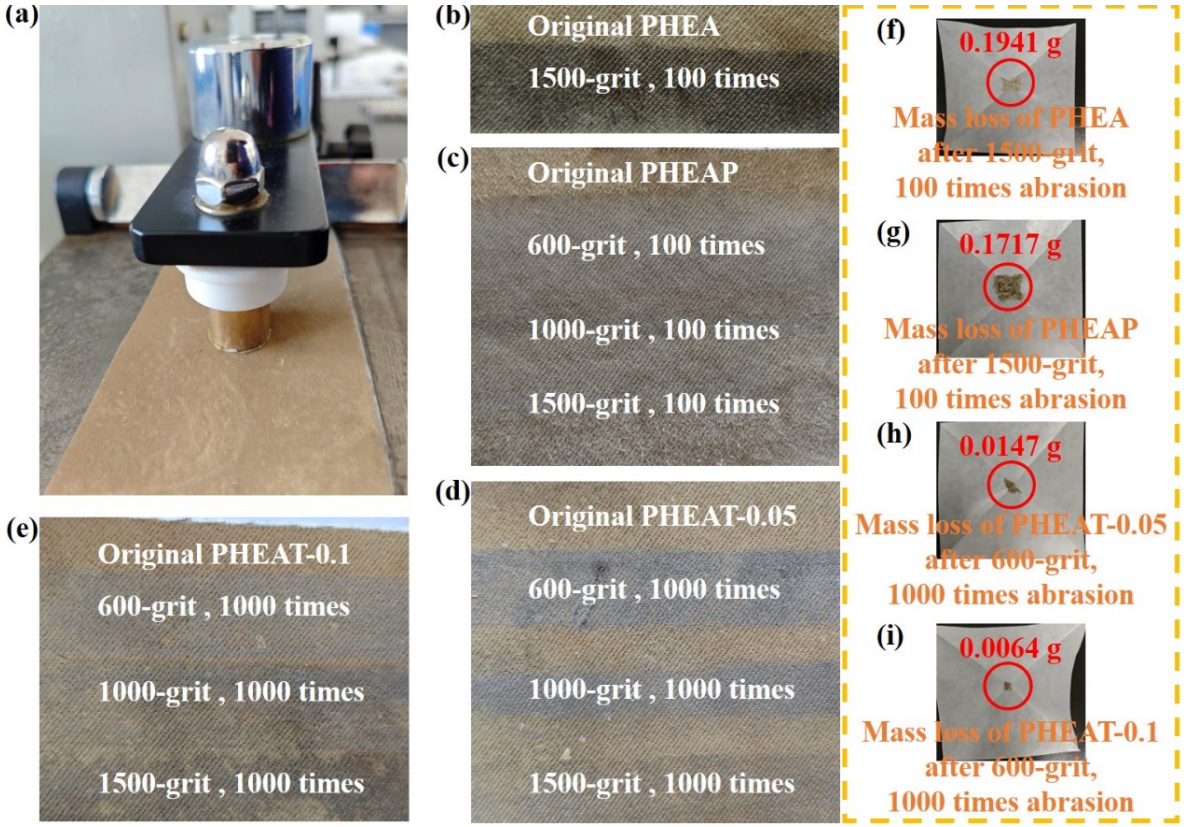


**Figure S4.** Abrasion resistance test. (**a**) A digital picture of the measurement setup; (**b**–**e**) Optical images of PHEA, PHEAP, PHEAT-0.05, and PHEAT-0.1 before and after sandpaper abrasion; (**f**–**i**) Mass loss of PHEA, PHEAP, PHEAT-0.05, and PHEAT-0.1 after abrasion.

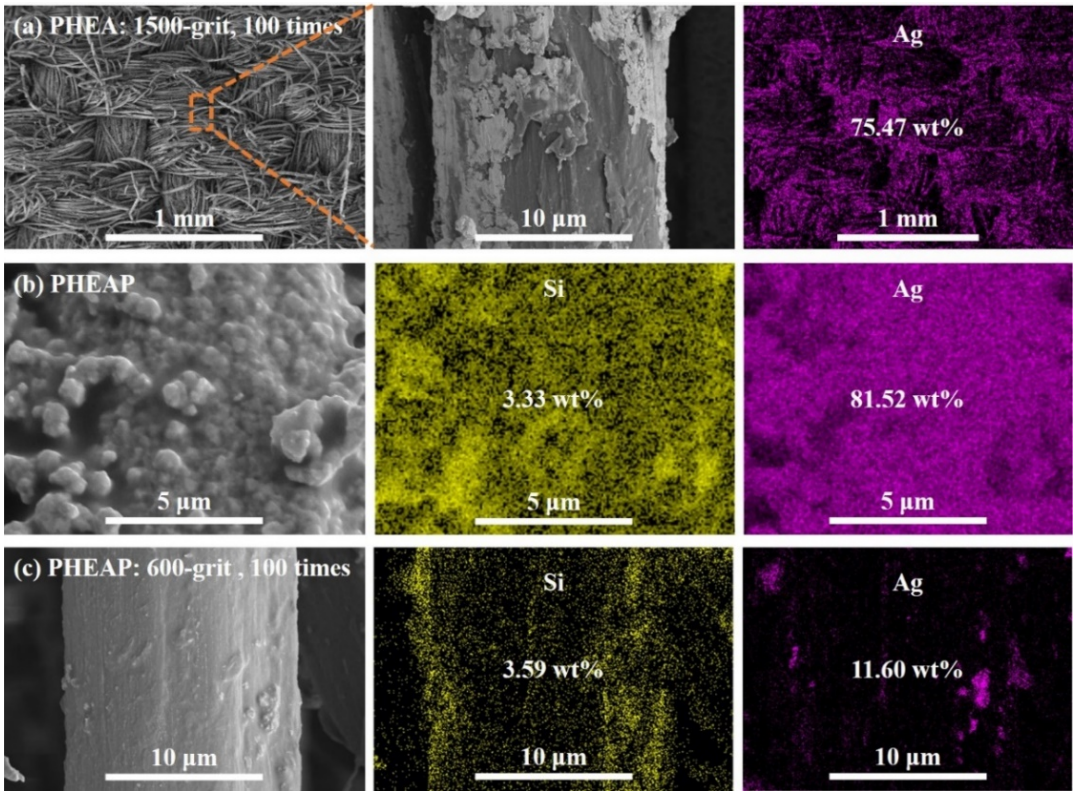


**Figure S5.** Microstructure of PHEA and PHEAP. SEM photographs and elemental mappings of (**a**) PHEA after abrasion test, PHEAP before (**b**) and after (**c**) abrasion test.

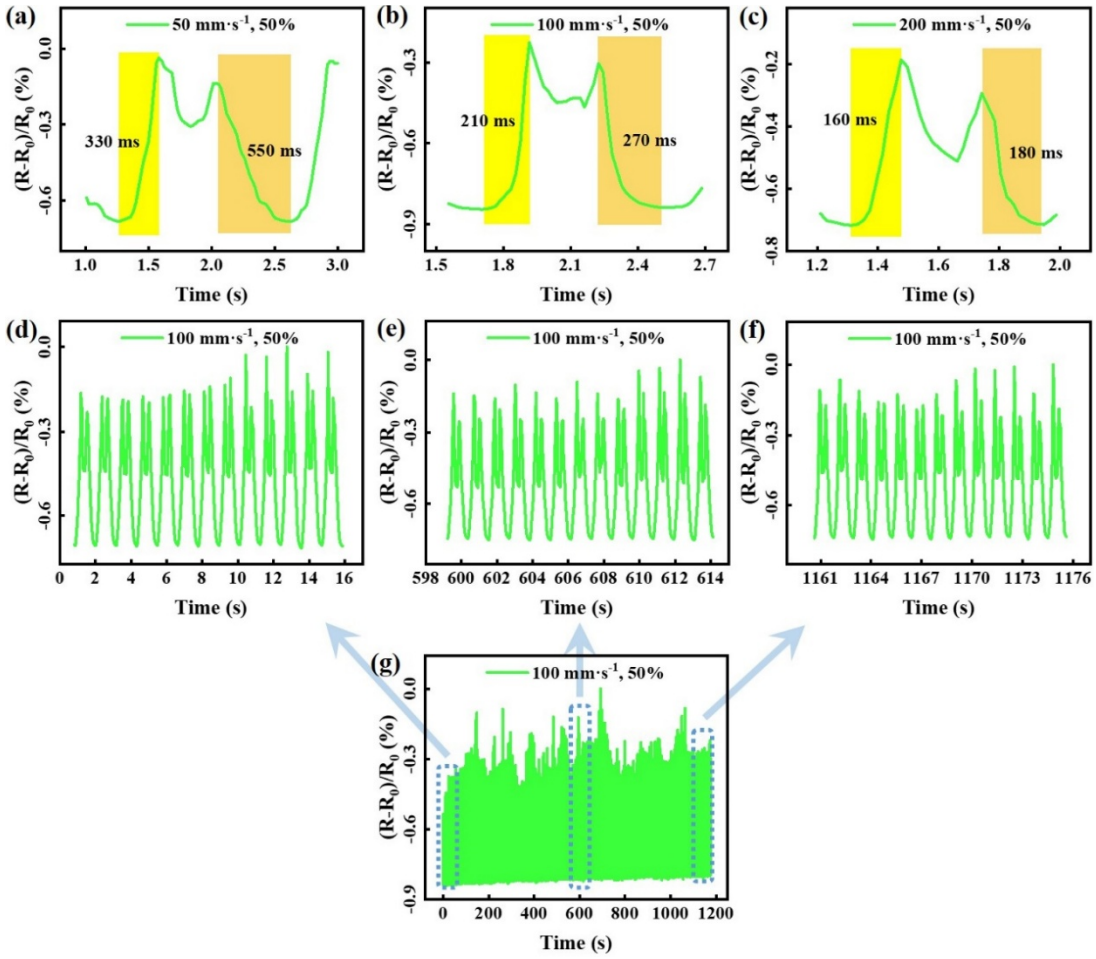


**Figure S6.** Sensing performance of PHEAT-0.05. (**a**–**c**) Response speed of the PHEAT-0.05; (**d**–**f**) Durability of PHEAT-0.05 over 1000 cycles.

**Table S1.** Summary of sample codes and abbreviations.

| Codes | Complete Name | Abbreviations | Complete Name |
|---|---|---|---|
| PMIA | Meta-aramid | EMI | Electromagnetic interference |
| HPAMAM | Hyperbranched polyamidoamine | EMW | Electromagnetic wave |
| EGDE | Ethylene glycol diglycidyl ether | $SE_T$ | Total shielding effectiveness |
| Ag | Silver | $SE_{\%}$ | Shielding efficiency |
| PDMS | Polydimethylsiloxane | $SE_A$ | Absorption effectiveness |
| TPU | Thermoplastic polyurethane | $SE_R$ | Reflection effectiveness |
| PHE | PMIA/HPAMAM-EGDE | *T* | Transmission coefficient |
| PHEA | PMIA/HPAMAM-EGDE/Ag | *A* | Absorption coefficient |
| PHEAP | PMIA/HPAMAM-EGDE/Ag/PDMS | *R* | Reflection coefficient |
| PHEAT | PMIA/HPAMAM-EGDE/Ag@TPU | *RCS* | Radar cross-section |
| PHEAT-X | X is the thickness of the TPU prior to hot-pressing | CST | Computer simulation technology |
| CPFCs | Conductive polymer fabric-based composites | PEC | Perfect electric conductor |

**Table S2.** A comprehensive comparison of $SE_T$, density, and the thickness of state-of-the-art CPFCs.

| Materials | $SE_T$ (dB) § | Density ($g \cdot cm^{-3}$) | Thickness (μm) | Ref. † |
|---|---|---|---|---|
| $Fe_3O_4$/Ag-loaded polyimide | 77 | 0.55 | 2460 | [5] |
| MXene/CuNWs@cotton | 53.2 | - | 1638 | [22] |
| PLA/P34HB/PEG/CNTs | 20.7 | - | 220 | [28] |
| $Ti_3C_2T_X$@ZnO@carbon | 29 | 0.279 | 768 | [29] |
| LM/CNT/ZAF-5/polyimide | 57.5 | 0.58 | 450 | [30] |
| AgNWs/MXene/graphene cotton | 77.5 | 0.686 | 1400 | [31] |
| SiC@C/carbon | 51.5 | - | 340 | [32] |
| TPU/PDA/AgNW/MXene | 91.9 | 0.125 | 2000 | [33] |
| Kevlar activated carbon | 28.5 | 0.1475 | 1400 | [34] |
| PHEAT-0.05 | 101.57 | 1.2 | 500 | This work |
| PHEAT-0.1 | 73.94 | 1.4 | 520 | This work |

§ For the X-band. † Since 2025. In the main text.

**Table S3.** A comprehensive comparison of abrasion resistance performance.

| Samples | Abrasion Cycles | Ag Content (wt%) before Abrasion § | Ag Content (wt%) after Abrasion § | $SE_T$ (dB) before Abrasion † | $SE_T$ (dB) after Abrasion † | $SE_T$ Retention (%) | Mass Loss (g) * | Strength (MPa) |
|---|---|---|---|---|---|---|---|---|
| PHEA | 100 (1500-grit) | 84.46 | 75.47 | 107.66 | 34.12 | 31.69 | 0.1941 | 40.4 |
| PHEAP | 100 (1500-grit) | 81.52 | 11.6 | 103.79 | 46.37 | 44.68 | 0.1717 | 69 |
| PHEAT-0.05 | 1000 (600-grit) | 2.63 | 20.24 | 101.57 | 52.95 | 52.13 | 0.0147 | 42.1 |
| PHEAT-0.1 | 1000 (600-grit) | 1.22 | 9.11 | 73.94 | 59.63 | 80.65 | 0.0064 | 49.8 |

§ From EDS data. † For the X-band. * From Figure S4f–i.

**Table S4.** A comparison of sensing performance with representative CPFCs strain sensors reported in recent literature.

| Materials | Response Time (ms) | Recovery Time (ms) | Ref. † |
|---|---|---|---|
| SEBS/Ga-In LM/Ag | 980 | 740 | [41] |
| PU/MXene/AgNPs | 355 | 722 | [42] |
| PPy/cotton | 1800 | 2400 | [43] |
| TA/MXene/DA | 89 | 79 | [44] |
| Microfluidic-directed polymer/hydrogel fabric | 429 | 590 | [45] |
| PEDOT@Nylon | 160 | 380 | [46] |
| MWCNT/PEDOT:PSS-coated crepe bandage | 237 | 63 | [47] |
| Hierarchical spiral-wrapped yarns | 170 | 182 | [48] |
| PET/APTES-PSA@Cu | 800 | 300 | [49] |
| PHEAT-0.05 (50 $mm \cdot s^{-1}$) | 330 | 550 | This work |
| PHEAT-0.05 (100 $mm \cdot s^{-1}$) | 210 | 270 | This work |
| PHEAT-0.05 (200 $mm \cdot s^{-1}$) | 160 | 180 | This work |

† Since 2025.